

An alternative copper electrowinning process based on reactive electro dialysis (RED)

Gerardo Cifuentes⁽¹⁾, Jaime Simpson⁽¹⁾, Francisco Lobos⁽¹⁾, Leoncio Briones⁽²⁾ and Alejandro Morales⁽³⁾.

⁽¹⁾ Departamento de Ingeniería Metalúrgica, Facultad de Ingeniería, Universidad de Santiago de Chile, Avenida Libertador Bernardo O'Higgins 3363, Casilla 10233, Fono: 56-2-7183224, Santiago, Chile. E-mail: gerardo.cifuentes@usach.cl.

⁽²⁾ Departamento de Ingeniería Mecánica, Facultad de Ingeniería, Universidad de Santiago de Chile.

⁽³⁾ Departamento de Ingeniería Metalúrgica, Universidad Católica del Norte. Avenida Angamos 0610, Antofagasta, Chile

This paper shows the preliminary results of an alternative to the classic electrowinning copper process using a cell based on reactive electro dialysis, which consists of two compartments separated by an anionic membrane, one of which contains the copper sulphate catholyte, where the cathode is located, and the other compartment contains the ferrous sulfate anolyte, where the anode is located. In this type of cell the anodic reaction is the oxidation of iron (Fe^{2+} to Fe^{3+}), which consumes less energy than the classic water oxidation. Moreover, this new anodic reaction does not produce acid mist.

Keywords: Copper, electrowinning, electro dialysis.

1. Introduction

The conventional copper electrowinning process, in spite of its present extensive use, has some drawbacks that over the last 20 years have been attempted to be overcome¹, but there are few implementations at the industrial level. These deficiencies are related mainly to the low electrolyte flow, whose direct consequence is a low efficiency of the mass transport phenomena. Furthermore, the specific surface area of the electrodes is low, and therefore the amount of mass deposited by chemical reaction is also low, and finally, among the drawbacks, there is a high energy requirement² (see Table 1.1) because the dominant reaction is the anodic decomposition of water, whose standard potential referred to the normal hydrogen electrode (NHE) is $E^\circ = 1.23$ V. As a direct consequence of this reaction, acid mist is also produced by the action of the generated oxygen which drags electrolyte along its path. To prevent all these phenomena that occur during conventional electrowinning, anodic reactions other than that of water have been proposed, such as, for example: Co/Co^{+3} ($E^\circ = 0.42$ V_{NHE}), I/I^- ($E^\circ = 0.54$ V_{NHE}), Ag/Ag^+ ($E^\circ = 0.80$ V_{NHE}), Pb/Pb^{+4} ($E^\circ = 0.77$ V_{NHE}), Hg/Hg^{+2} ($E^\circ = 0.85$ V_{NHE}), and the $\text{Fe}^{+2}/\text{Fe}^{+3}$ ($E^\circ = 0.77$ V_{NHE}), and $\text{Hg}_2^{+2}/\text{Hg}^{+2}$ ($E^\circ = 0.92$ V_{NHE}) redox couples.^{3,4} Any of the above reactions can decrease the total energy of the copper electrowinning cell if the following basic conditions are fulfilled: that the algebraic sum of their Nernst

equilibrium potentials ($E_{\text{cathode}} - E_{\text{anode}} = \Delta E_{\text{eq}}$) and the anodic overpotential are less than those that consider the evolution of oxygen from the oxidation of water, thereby having as a direct consequence a low cost due to energy savings and less impact on the work areas due to the elimination of acid mist.⁵ One of the most promising reactions is the transformation of ferrous to ferric ion mentioned above.^{6,7} One way of preventing the reverse reaction (from ferric to ferrous) from taking place at the cathode and thereby affecting the faradic cathodic efficiency, consists in using two electrolytes (anolyte and catholyte) instead of only one, retaining the conductivity between them.^{8,9,10,11,12} This is possible using an electrodialysis membrane to separate those electrolytes in order to obtain specific electrode reactions. This process is known as reactive electrodialysis (RED). In this context it must also be considered that the sum of the resistances of the catholyte, the anolyte, and the membrane is not greater than the decrease achieved by changing the anodic reaction as well as by decreasing the corresponding overpotential.¹³

Table 1.1.- Distribution of potential in conventional electrowinning

Parameter	Volts	%
ΔE_{eq} = Equilibrium potential dif.	0.9	42.8
$ \eta_a $ = Anodic overpotential	0.5	23.8
η_c = Cathodic overpotential	0.05	2.4
$I \cdot R_e$ drop in the electrolyte at 200 A/m ²	0.5	23.8
Loss from contact	0.15	7.2
V_{cell} = Total cell voltage	2.1	100.0

Table 1.1 can be represented in mathematical terms, with the potential difference that is produced in the conventional electrowinning cell expressed by

$$V_{\text{cell}} = E + I \cdot R_e \quad (1)$$

where $E = \Delta E_{\text{eq}} + \eta_a + |\eta_c|$. This differs with respect to the cell potential expression associated with a RED process that considers the following terms:

$$V_{\text{cell}} = \Delta E_{\text{eq}} + \eta_a + |\eta_c| + I \cdot (R_a + R_c + R_m) \quad (2)$$

where R_a , R_c and R_m are the resistances associated with the anolyte, catholyte, and membrane, respectively. The above expressions do not consider losses associated with electronic contacts and/or conductors. On the other hand, the specific energy consumption (W) for any copper electrolysis cell is given by:

$$W = \frac{V_{\text{cell}} \cdot I \cdot t}{M_{\text{deposited copper}}} \quad (3)$$

where I is the current fed and t is electrolysis time, usually in amperes and hours, respectively. M is the copper deposited on the cathode.

Most industrial electrolytic processes in the copper speciality work under mass transfer control. If diffusion, J_D , is the transport mechanism and using Fick's law of diffusion too, the flux equality condition becomes:

$$\frac{i}{n \cdot F} = J_D = -D \cdot \left(\frac{dc}{dx} \right)_{x=0} \quad (4)$$

where i is the current density, n is the electrons transferred, F is Faraday's constant and D is the diffusional coefficient. In general, this concentration profile is such that there is a linear variation of concentration over small distances from the interface and then the concentration asymptotically approaches the bulk value c^0 . Nernst put forward a simplifying suggestion, extrapolating the linear part of the concentration-versus-distance curve until it intersects the bulk value of the concentration at some distance δ from the interface. Then, the concentration gradient at $x=0$, i.e., $(dc/dx)_{x=0}$, can be replaced by $(c^0 - c_{x=0})/\delta$ to give:

$$\frac{i}{n \cdot F} = J_D = -D \cdot \left(\frac{c^0 - c_{x=0}}{\delta} \right) \quad (5)$$

where $c_{x=0}$ is the concentration at the electrode interface. Therefore, each overpotential present in equations (1) and (2) can be written separately as:

$$\eta = \eta_{TC} + \eta_D \quad (6)$$

here η_{TC} and η_D are the transport charge and diffusional overpotential, respectively.

In this approximation, therefore, one can consider that the diffusion occurs across a region parallel to the electrode interface, i.e., across a Nernst diffusion layer of effective thickness δ . The precise value of the above diffusion layer depends largely on the effectiveness of forced convection, and is smaller the greater the effectiveness is. Generally, convection is laminar where the value of δ and hence of the concentration gradient is governed by the electrode geometry, the kinematic viscosity, the diffusion coefficient, and the velocity of the liquid caused by stirring; turbulent flow is also usually involved when the electrolyte is stirred. Both types of convection have been described by Levich¹. There are studies related to the process of electroanalysis associated with copper, but they are still confusing and contradictory.^{14,15,16} An important aspect is that related to operational flow, which causes great expectation because if work can be done with greater flows, higher limiting currents would be obtained as a consequence of higher current density, leading to the same copper production with a much smaller infrastructure. Reactive electroanalysis applied to the electrowinning of copper is a vision of the future in the present.

This paper attempts to demonstrate that copper electrowinning based on reactive electroanalysis can be a good alternative process compared to the present electrowinning process in terms of specific energy, cell voltage, and current density.

2. Experimental part

Figure 2.1 presents the experimental scheme and the cell used in this work.

The effective catholyte and anolyte volumes in the compartment were 275 cm³ of each, adding up to a total volume of 550 cm³, because both electrolytes were recirculated with peristaltic pumps at flows of 700, 800, 900 and 1,200 cm³/min. The electrolyte's working temperatures were 40, 50 and 60 °C. The cathode consisted of a 4 cm² copper sheet and the anode was made of platinum, with their back sides insulated with teflon. The cathode current densities used were 300, 450 and 600 A/m². A 2x2 cm Ionac MA3475 anionic membrane was used as the separation medium between the two

electrolyte compartments. This membrane was attached to the separating frame by means of rubber gaskets.

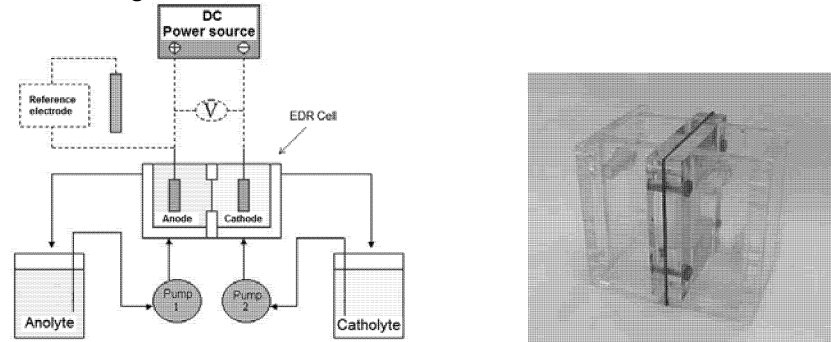


Figure 2.1- Experimental scheme of RED (left) and the cell (right) used in in this study.

The composition of the anolyte was 190 g/L of H_2SO_4 and a 1M concentration of Fe^{2+} (as $\text{FeSO}_4 \cdot 7\text{H}_2\text{O}$). The composition of the catholyte was 190 g/L of H_2SO_4 and 30 g/L of Cu^{2+} as $\text{CuSO}_4 \cdot 5\text{H}_2\text{O}$). Electrolysis time for all the tests was 2 hours.

3. Results and discussion

3.1 Effect of electrolyte flow

From all the results presents in this work, except at 600 A/m^2 , it is seen that as electrolyte flow in the cell increases, there is a decrease of the corresponding potential difference. This can be explained graphically with an Evans diagram, shown in Figure 3.1, where for a fixed current density, for example, cell potential decreases as electrolyte flow (Q_i) in the cell increases.

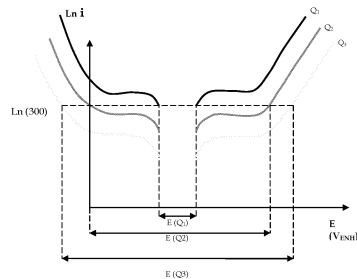


Figure 3.1.- Explanatory Evans diagram for different electrolyte flows (Q_i) at the same current density of 300 A/m^2 , where: ($Q_1 \cdot Q_2 \cdot Q_3$).

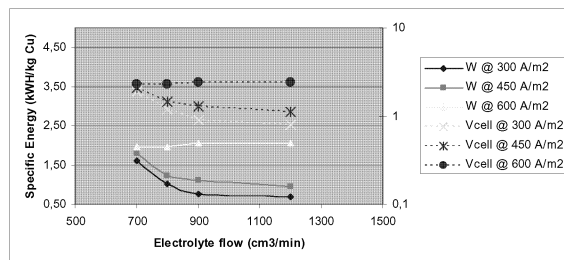


Figure 3.2.- Effect of electrolyte flow on specific energy and electrolyte flows (Q_i) at the same current density V_{cell} (right log y axis) at different current densities at $40 \text{ }^\circ\text{C}$.

In fact, if we work at a constant temperature of $40 \text{ }^\circ\text{C}$ and a current density of 300 A/m^2 , see Figure 3.2, we get a cell potential of 1.9 V for $700 \text{ cm}^3/\text{min}$, 1.2 V for $800 \text{ cm}^3/\text{min}$, 0.9 V for $900 \text{ cm}^3/\text{min}$, and 0.8 V for $1,200 \text{ cm}^3/\text{min}$, all of them lower than the conventional cell potentials shown in Table 1.1. Moreover, in Figure 3.2 it is seen that at 600 A/m^2 the specific energy (W) is practically constant at different electrolyte flows, because for this system V_{cell} and the deposited copper are constant too (see Equation

(3)). On the other hand, at 300 and 450 A/m² the value of W decreases when electrolyte flow increases, and this effect is directly proportional to the V_{cell} decrease described above, because η_a and η_c in Equation (2), particularly η_D of each one, Equation (6), decreases because the concentration gradient and δ at the electrodes also decrease, and therefore J_D is favored (see Equation (5)).

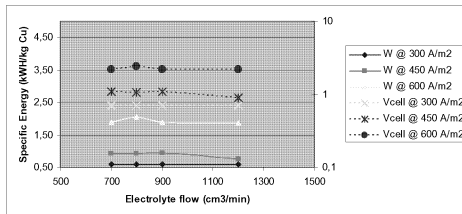


Figure 3.3.- Effect of electrolyte flow on specific energy and V_{cell} (right log y axis) at different current densities at 50 °C.

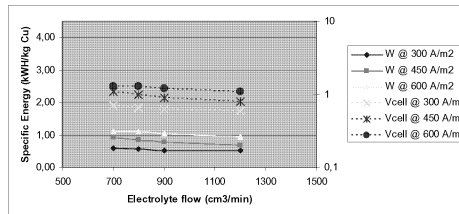


Figure 3.4.- Effect of electrolyte flow on specific energy and V_{cell} (right log y axis) at different current densities at 60 °C.

Figures 3.3 and 3.4 show that specific energy and V_{cell} show a slight decrease with respect to the result of Figure 3.2 at 40 °C, and at higher temperature as shown in Figure 3.4, produced the lowest specific energy and cell potential values of all the current densities tested.

3.2 Effect of temperature

When the work was done at constant electrolyte flow and the temperature increase, a decrease of the cell potential is seen that increases as the flow decreases, showing that as the forced convection conditions in the proximity of the membrane improve, polarization due to concentration close to it is minimized, thereby decreasing the cell's energy expenditure.

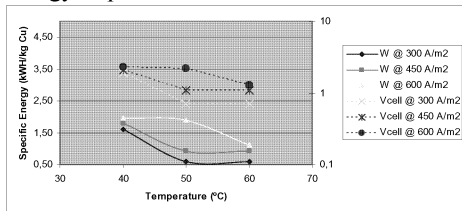


Figure 3.5.- Effect of temperature on specific energy and V_{cell} (right log y axis) at diff. current densities at 700 cm³/min.

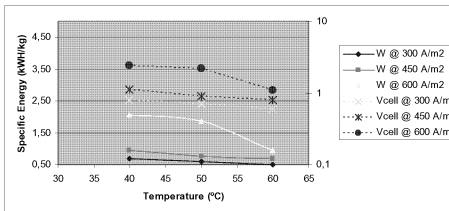


Figure 3.6.- Effect of temperature on specific energy and V_{cell} (right log y axis) at diff. current densities at 1,200 cm³/min.

3.3 Effect of current density

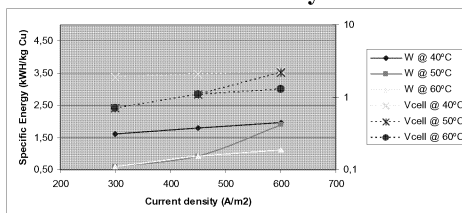


Figure 3.9.- Effect of current density on specific energy and V_{cell} (right log y axis) at diff. temperatures at 700 cm³/min.

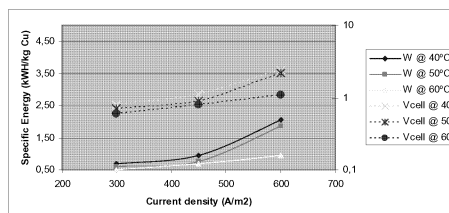


Figure 3.10.- Effect of current density on specific energy and V_{cell} (right log y axis) at diff. temperatures at 1,280 cm³/min.

As expected, an increase in current density implies an increase of the system's cell potential (see Equation 2), but this increase is less significant at an electrolyte temperature of 60 °C at all electrolyte flows, and particularly at 1,200 cm³/min V_{cell} is minimum (see Figure 3.12) compared to the results shown in Figures 3.9 to 3.11. The average faradic cathodic efficiency for all the tests was 98.68%, i.e., no change was detected in the current efficiency under all the conditions tested.

4. Conclusions

Using RED, cell potential and specific energy are decreased with respect to the traditional copper electrowinning system, with a maximum six-fold difference between both processes. In all the tests the average current efficiency was 98.68%, i.e., no change was detected in the current efficiency under all the conditions tested. The parameters studied here confirm an important aspect of this study is that related to operational flow, which causes great expectation because if work can be done at greater flows, higher limiting currents would be obtained as a consequence of a higher current density, leading to the same copper production with a much smaller infrastructure, high current efficiency, and low specific energy.

Acknowledgements

The authors acknowledge the support of the Comisión Nacional de Investigación Científica y Tecnológica under FONDEF project D97I2035 and the Universidad de Santiago de Chile, USACH.

References

- 1- J.O'M. Bockris, A.K.N. Reddy, *Modern electrochemistry*, Plenum Press, New York, **1**, (1977).
- 2- A.K. Biswas, W.G. Davenport, *Extractive Metallurgy of Copper*, third edition, Pergamon Press, Oxford, (1994).
- 3- J.M. Casas, F. Alvarez, L. Cifuentes, *Chem. Eng. Sc.*, **55**, 6223, (2000).
- 4- L. Cifuentes, R. Glasner, G. Crisóstomo, J.M. Casas in *Procs. Copper 2003, International Conference*, J.E. Dutrizac, C.G. Clement eds. Canadian Institute of Mining, Metallurgy and Petroleum, Montreal, 623, (2003).
- 5- J. Menacho in *First Meeting on Minor Element Contaminants in Copper Metallurgy*, J. Álvarez, R. Padilla, R. Parra, M. Sánchez, F. Vergara, eds., Universidad de Concepción, 169, (2007).
- 6- J.M. Casas, G. Crisóstomo, L. Cifuentes, *Hydrometallurgy*, **80**, **4**, 254-264, (2005).
- 7- L. Cifuentes, G. Crisóstomo, J.P. Ibáñez, J.M. Casas, F. Alvarez, G. Cifuentes, *J. of Membrane Sc.*, **207**, **1**, (2002).
- 8- L. Cifuentes, R. Glasner, J.M. Casas, *Chem. Eng. Sci.*, **59**, **5**, 1087, (2004).
- 9- L. Cifuentes, C. Mondaca, J.M. Casas, *Minerals Engineering*, **17**, 803, (2004).
- 10- L. Cifuentes, R. Ortiz, J.M. Casas, *AIChE J.*, **51**, **8**, 2273, (2005).
- 11- L. Cifuentes, J. Simpson, *Chem. Eng. Sci.*, **60**, **17**, 4915, (2005).
- 12- L. Cifuentes, J.M. Castro, J.M. Casas, J. Simpson, *Applied Math.* Available On Line, (2006).
- 13- L. Cifuentes, J.M. Casas, J. Simpson, *Chem. Eng. Research and Design*. **84**, A10, 965, (2006).
- 14- D.C. Price, W.G. Davenport, *Metallurgical Transactions B*, **12B**, 639, (1981).
- 15- Y. Lorrain, G. Pourcelly, C. Gavach, *J. Membrane Sci.* **110**, 181, (1996).
- 16- Y. Lorrain, G. Pourcelly, C. Gavach, *Desalination*, **109**, 231, (1997).